

NMR Spectroscopy of Paramagnetic Complexes

Part 39*—Natural Abundance ^2H NMR of Paramagnetic Sandwich Compounds

Janet Blümel, Peter Hofmann and Frank H. Köhler†

Anorganisch-chemisches Institut, Technische Universität München, D-8046 Garching, Germany

The methylated metallocenes $(\text{MeCp})_2\text{M}$ with $\text{M} = \text{V}, \text{Cr}, \text{Mn}, \text{Co}, \text{Ni}$ (1–5) were investigated by ^1H and ^2H NMR spectroscopy at natural abundance. The ^2H NMR signals are narrower by a factor of up to 30 compared with the corresponding ^1H NMR signals, thus establishing an inexpensive method and a general improvement of the NMR spectra of paramagnetic π -complexes. This has allowed the resolution of the signal splitting of Cp deuterons of 1 and 5 which could not be observed earlier in the ^1H NMR spectra. The origin of the small (1 and 5) and large (2–4) signal splittings is discussed and related to an extended Hückel calculation. The relative magnitude of the signal splitting is reproduced, but the signal assignment had to be deduced from ^{13}C NMR results. Primary isotope shifts of up to 4.0 ppm were found for 1, 2, 4 and 5. The much higher values for 3 (up to 16.6 ppm) reflect the combined influence of the intrinsic isotope shift and the isotope effect on the spin crossover.

KEY WORDS Paramagnetic NMR Natural abundance ^2H NMR ^2H signal narrowing ^2H isotope effect EHMO calculation

INTRODUCTION

The use of ^2H instead of ^1H NMR spectroscopy has led to considerable progress in the characterization of paramagnetic organometallic compounds. In general, the signal half-width at a given temperature, W_T , is much smaller for ^2H NMR signals, and for the metallocenes $(\text{C}_5\text{H}_5)_2\text{M}$ and $(\text{C}_5\text{D}_5)_2\text{M}$ the theoretical factor of $W_T(^1\text{H})/W_T(^2\text{H}) = 42$ has been attained.¹ This effect has been applied to detect deuterons which are located so close to the paramagnetic metal centre of a complex that the corresponding ^1H NMR signal is broadened beyond detection.² Further, the spin crossover and the dimerization of manganocene could be clarified by using ^2H NMR spectroscopy.³

The line narrowing effect is, of course, related to an improved spectral resolution. In this work we wanted to test this for the bis(methyl- η^5 -cyclopentadienyl)metal derivatives $(\text{MeCp})_2\text{M}$ because, for the series $\text{M} = \text{V}, \text{Cr}, \text{Mn}, \text{Co}, \text{Ni}$ (1–5), a surprising metal-dependent signal splitting arises. For instance, less ^1H NMR signals than expected from symmetry have been observed when $\text{M} = \text{V}$ and Ni, and it was unclear whether this originated from resolution problems or whether the theory had to be modified.⁴ Because of the low receptivity of the deuteron and the large signal width encountered for paramagnetic molecules, deuterium-enriched samples had to be used in previous investigations.^{1–3} Here we demonstrate that the method is not necessarily expensive, because deuterium at the

natural abundance level may be sufficient. Further, we demonstrate that the qualitative molecular orbital concept used for the general understanding of the NMR results of paramagnetic π -complexes is also instrumental in accounting for the peculiarities outlined below.

RESULTS

The liquid 1,1'-dimethylmetallocenes 1–5 gave good ^2H NMR spectra within an acceptable accumulation time. A typical example is the spectrum of 5 in Fig. 1, which was obtained after 3.5 h. This shows that less concentrated samples and/or a shorter recording time are adequate. The signal half-width $W_T(^2\text{H})$ is considerably smaller than $W_T(^1\text{H})$ for all compounds (cf. Table 1). In the case of 5 this leads to signals of D-2–5 that are well separated (Fig. 1, inset A), whereas only one signal

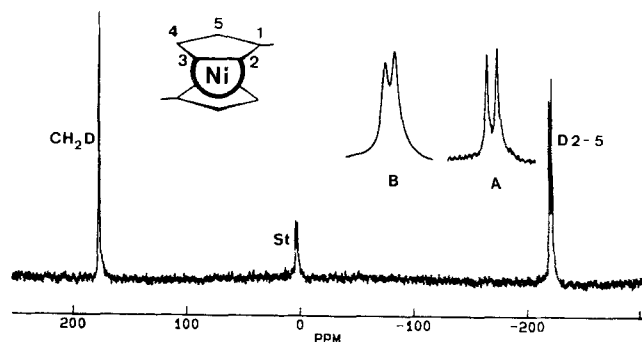


Figure 1. 46 MHz ^2H NMR spectrum of a mixture of $(\text{MeCp})_2\text{Ni}$ and $(\text{MeCp})_2\text{Fe}$ (St, internal standard) at 338 K. The scale is given arbitrarily relative to $(\text{MeCp})_2\text{Fe}$. Inset: signals of D-2–5 at (A) 46 MHz and (B) H-2–5 at 300 MHz expanded by a factor of 9.

* For Part 38, see Ref. 3.

† Author to whom correspondence should be addressed.

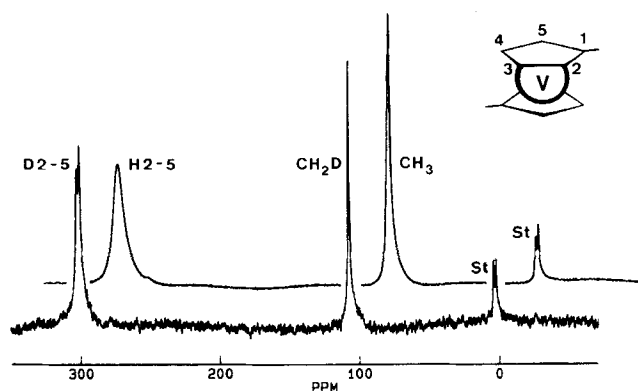


Figure 2. (Top) 300 MHz ^1H and (bottom) 46 MHz ^2H NMR spectra of a mixture of $(\text{MeCp})_2\text{V}$ and $(\text{MeCp})_2\text{Fe}$ (St, internal standard) at 338 K. Scale as in Fig. 1 and only for the ^2H NMR spectrum.

appears for H-2-5 at 200 MHz.⁴ The signals of H-2-5 could be partly resolved by changing from 200 to 300 MHz, but the additional effect of ^2H signal narrowing is clearly visible in the inset in Fig. 1. For the corresponding vanadocene **1** only one signal could be observed for H-2-5 even at 300 MHz, whereas D-2/5 and D-3/4 were separated by 1.9 ppm in the ^2H NMR spectrum (Fig. 2).

The paramagnetic signal shifts $\delta^{\text{para}}(^2\text{H})$ and, for comparison, $\delta^{\text{para}}(^1\text{H})$ were determined directly by referencing relative to the corresponding signals of internal $(\text{MeCp})_2\text{Fe}$. These are shown together with other data in Table 1. Since both the ^2H and ^1H NMR spectra were obtained from the same sample at the same temperature (see Experimental), concentration-dependent intermolecular⁵ and temperature effects on the shifts could be excluded, so that the shift differences between analogous ^1H and ^2H NMR signals are primary isotope effects $\Delta_{\text{p}}^{\text{para}}(^2/1\text{H}) = \delta^{\text{para}}(^1\text{H}) - \delta^{\text{para}}(^2\text{H})$.

DISCUSSION

Origin of the signal splitting

There is a striking difference in the signal splitting of the Cp protons within the series $(\text{MeCp})_2\text{M}$: for $\text{M} = \text{Cr}$,

Mn and Co (**2**, **3** and **4**) it is large, whereas for $\text{M} = \text{V}$ and Ni (**1** and **5**) it is very small. For the understanding of these results an approach is desirable that is applicable for all $(\text{MeCp})_2\text{M}$ compounds, with slight modifications depending on the metal. Such an approach is MO theory combined with perturbation theory arguments, as illustrated in Fig. 3. Although calculated for $(\text{MeCp})_2\text{Ni}$, the scheme in Fig. 3B is useful for all $(\text{MeCp})_2\text{M}$ compounds because, as shown below, only e_1 -type orbitals need be considered.

Starting from the Cp π -orbitals, substitution by a methyl group lifts the orbital degeneracy and places the symmetric e_1 orbital ($s\text{-}e_1$) above the antisymmetric orbital ($a\text{-}e_1$) (Fig. 3A), similar to the situation in toluene.⁶ The same applies for the e_2 orbitals. When two $[\text{MeCp}]^-$ ligands are arranged parallel to each other at the distance found in metallocenes we obtain $[\text{MeCp}]_2^{2-}$ with further level splitting. Although here [and for $(\text{MeCp})_2\text{M}$ in Fig. 3B] the symmetry is C_{2h} , the levels have been labelled as a , e_1 and e_2 for simplicity in order to maintain the relationship to unperturbed D_{5h} or D_{5d} metallocenes. An EHMO calculation provides a guide for these level splittings: $[\text{MeCp}]^-$, e_1 0.22 eV, e_2 0.12 eV; $[\text{MeCp}]_2^{2-}$ with a ligand separation of 3.60 Å, e_1 0.17/0.23 eV, e_2 0.10/0.14 eV. Note that the e_1 orbitals of $[\text{MeCp}]_2^{2-}$ which are appropriate for the interaction with metal 3d orbitals still have $s\text{-}e_1$ above $a\text{-}e_1$.

The diagram in Fig. 3B only shows those π -orbitals of $[\text{MeCp}]_2^{2-}$ which interact with the metal valence AOs (3d, 4s, 4p). The result of the interaction is the well known two-above-three level pattern of metallocenes. The bonding e_1 orbitals are also given in Fig. 3B, whereas levels of σ symmetry and π -group MOs of $[\text{MeCp}]_2^{2-}$, which only interact with metal 4p AOs, have been omitted for clarity.

Cobaltocene. We have shown previously⁷ that if only one unpaired electron is present in the e_1^* set, as is the case in $(\text{MeCp})_2\text{Co}$, it will strongly prefer the lower of the two e_1^* components. Let us suppose that as in Fig. 3B it is the one containing the $a\text{-}e_1$ contribution of the ligand and the d_{xz} metal AO. We then follow qualitatively the squared carbon $2p_z$ orbital coefficients, which

Table 1. $^2/1\text{H}$ NMR data^a for paramagnetic 1,1'-dimethylmetallocenes ($\text{M} = \text{V}, \text{Cr}, \text{Mn}, \text{Co}, \text{Ni}; 1\text{-}5$) at 338 K

Compound	Nucleus	$^1/2\text{H}\text{-}2/5$			$^1/2\text{H}\text{-}3/4$			$\text{C}^1/2\text{H}_3$		
		δ^{para}	W	$\Delta_{\text{p}}^{\text{para}}$	δ^{para}	W	$\Delta_{\text{p}}^{\text{para}}$	δ^{para}	W	$\Delta_{\text{p}}^{\text{para}}$
1	^1H	301.1	2750	0.8	301.1	2750	2.7	109.2	710	1.9
	^2H	300.3	100		298.4	94		107.3	26	
2	^1H	327.7	2330	1.9	280.4	2040	1.6	31.9	340	0.6
	^2H	325.8	71		278.8	66		31.3	18	
3	$^1\text{H}^{\text{b}}$	4.7	3960	0	80.5	8100	6.7	144.4	10850	16.6
	$^2\text{H}^{\text{c}}$	4.7	320		73.8	410		127.8	540	
4	^1H	-60.8	290	0	-41.8	220	-0.1	14.4	56	0.5
	^2H	-60.8	9		-41.7	9		13.9	6	
5	^1H	-221.2	460	0.2	-223.0	810	0.3	181.1	270	4.0
	^2H	-221.4	25		-223.3	27		177.1	17	

^a Paramagnetic shifts, δ^{para} (± 0.1 ppm), and isotope shifts, $\Delta_{\text{p}}^{\text{para}}$, in ppm, negative sign for shifts to low frequency; signal half-width W in Hz.

^b ± 0.5 ppm owing to overlapping or broad signals.

^c ± 1.0 ppm owing to overlapping or broad signals.

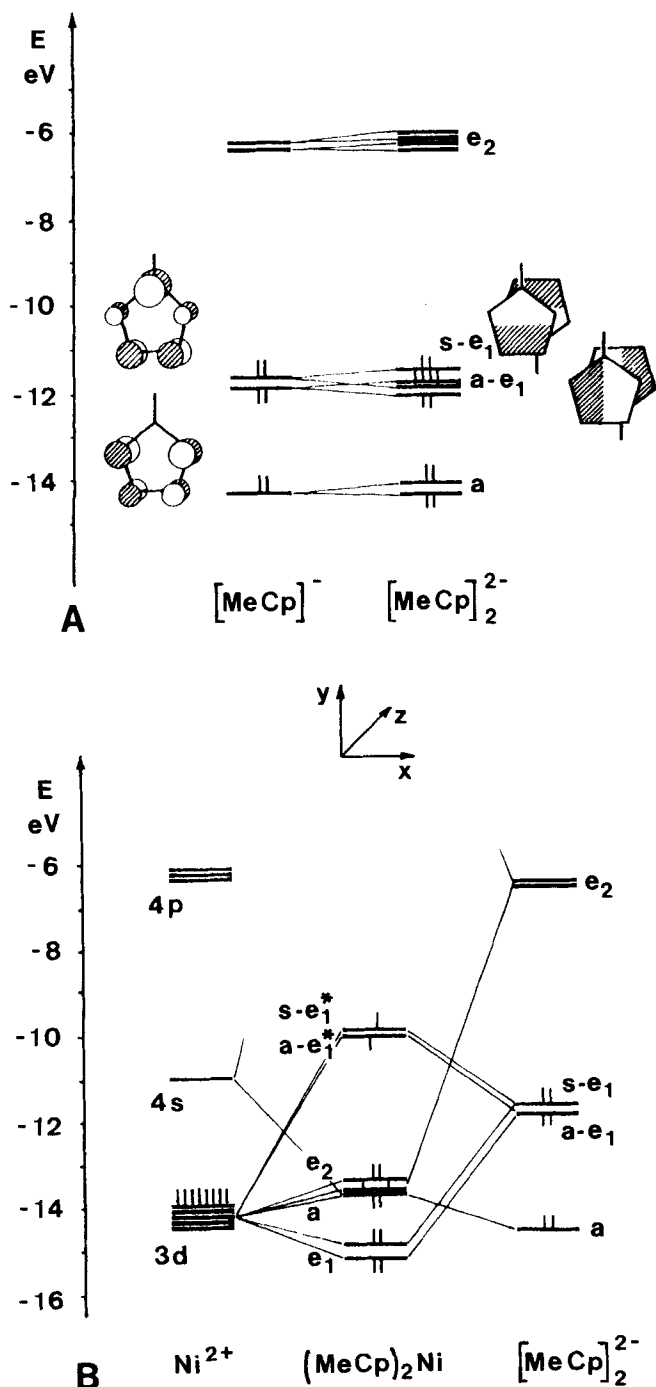


Figure 3. (A) MO diagram for the π -orbital interaction of two $[\text{MeCp}]^-$ ligands at the distance found in Cp_2Ni . For labelling, see text. (B) MO diagram for the important metal-ligand π -interactions in $(\text{MeCp})_2\text{Ni}$.

in simple cases are a good measure of the spin density and thus of the hyperfine coupling constants $A(^1\text{H})^8$ and $A(^{13}\text{C})^9$. Since $A(^1\text{H}/^{13}\text{C})$ is proportional to the corresponding NMR signal shifts, the signal of H-2/5 should be much more shifted than that of H-3/4. This is in accord with the ^{13}C NMR result showing $\delta^{\text{para}}(\text{C-1}) < \delta^{\text{para}}(\text{C-3/4}) < \delta^{\text{para}}(\text{C-2/5})^{4c,7c}$ and confirms the level ordering given in Fig. 3B.

Nickelocene. Since the splitting of the e_1^* orbitals is small, two unpaired electrons are present in $(\text{MeCp})_2\text{Ni}$ and both the $a-e_1$ and $s-e_1$ ligand orbitals are engaged

in the spin delocalization. Therefore, we have to add the $c_i^2(\text{C2 } p_z)$ values of the two orbitals, which yields very similar spin densities at all ring carbon atoms. An approximate idea is provided by the EHMO results for $[\text{MeCp}]^-$: C-1 0.351, C-3/4 0.359, C-2/5 0.389 (if only one e_1^* orbital were engaged the splitting would be much larger: C-1, C-3/4, C-2/5 with 0.351/0.230/0.052 for $a-e_1^*$ and with 0/0.129/0.337 for $s-e_1^*$). Qualitatively this reflects very well the fact that positions 3/4 and 2/5 can be distinguished only by the more powerful ^2H NMR spectroscopy. The signal assignment for D-2/5 and D-3/4 is simple when based on the ^{13}C NMR results, and when the spin distribution associated with either the $a-e_1^*$ or the $s-e_1^*$ orbital (Fig. 3) dominates the signal shifts. For $(\text{MeCp})_2\text{Ni}$ we found $\delta^{\text{para}}(^{13}\text{C}) = 1536$ (C-1), 1510 (C-3/4) and 1356 (C-2/5)¹⁰ (note that we have since changed the sign convention). It follows that the $s-e_1^*$ orbital dominates and that the signal of D-3/4 is more shifted than that of D-2/5.

The dominance of the $s-e_1^*$ orbital seems to be reflected in the results of an EHMO calculation on $(\text{MeCp})_2\text{Ni}$ (Fig. 3B) where we find a metal contribution of 30% for $a-e_1^*$ and of 28.4% for $s-e_1^*$ at 0.10 eV higher energy. The reason for this is that the overlap $\langle a-e_1/d_{xz} \rangle$ is larger than $\langle s-e_1/d_{yz} \rangle$. However, when the $c_i(\text{C2 } p_z)$ values of the two SOMOs are used to calculate the $A(^{13}\text{C})$ values according to Ref. 9b, the sequence of the ^{13}C NMR signals is opposite to the experimental result. The same is true if we correct the experimental result for the metal-centred dipolar shifts using the approach of Kurland and McGarvey¹¹ and the data of Baltzer *et al.*¹² and Seiler and Dunitz¹³ (-26.7 and -1.7 ppm for all carbon and hydrogen atoms of Cp, respectively) and for the ligand-centred dipolar shifts as described previously¹⁴ (35–38 ppm).

We conclude that, qualitatively, the NMR results for $(\text{MeCp})_2\text{Ni}$ are well understood. The best that can be stated for quantitative EHMO results is that they have a strong scatter, depending on the parameters. Actually, Rettig and Drago¹⁵ have calculated a π spin density sequence for $(\text{Cp})(\text{MeCp})\text{Ni}$ which is inverse to ours. Their sequence is inverted again when a correction is made for σ spin density.

Chromocene. The NMR spectra of $(\text{MeCp})_2\text{Cr}$ are similar to those of cobaltocenes in that the splitting of the resonances for C-1–5 and the corresponding protons of substituted Cp ligands is large.⁷ The reversal of the shift sign is due to a polarization step in which the unpaired electron in the e_2 orbitals ($^3E_{2g}$ ground state, i.e. e_2^3, a^1 , for Cp_2Cr ; cf. Fig. 3 with three electrons less) act on those in the e_1 orbitals. Therefore, one of the e_1 orbitals strongly dominates the spin delocalization. ^{13}C NMR spectroscopy shows^{4c,7c} that for $(\text{MeCp})_2\text{Cr}$ this is the $a-e_1$ orbital (the sequence of $|\delta^{\text{para}}(^{13}\text{C})|$ is $1 < 3/4 < 2/5$), so that in the present study the signal of D-2/5 must be more shifted than that of D-3/4.

Vanadocene. Vanadocene, with a $^4A_{2g}$ ground state (e_2^2, a^1 ; cf. Fig. 3B with four electrons less) for Cp_2V , shows NMR characteristics that are related to those of chromocenes and nickelocenes. The polarization of paired e_1 electrons by unpaired e_2 electrons leads to the

same signal shift signs as for chromocenes. However, both the $a-e_1$ and $s-e_1$ ligand orbitals are now concerned in $(\text{MeCp})_2\text{V}$ (via the metallocene e_1 orbitals) in a similar manner as in $(\text{MeCp})_2\text{Ni}$ (via the metallocene e_1^* orbitals), and the NMR signal splitting is so small that it can only be resolved by using ^2H NMR spectroscopy. In view of the problems encountered with $(\text{MeCp})_2\text{Ni}$ we renounced an EHMO calculation of $(\text{MeCp})_2\text{V}$ as a basis for the signal assignment of D-2-5. Instead, we followed the ^{13}C NMR result^{4c,7c} (the sequence of $|\delta^{\text{para}}(^{13}\text{C})|$ is $1 < 3/4 < 2/5$), which implies that the $a-e_1$ orbital is more important and that $\delta^{\text{para}}(^2\text{H}-2/5)$ is larger than $\delta^{\text{para}}(^2\text{H}-3/4)$.

Manganocene. For $(\text{MeCp})_2\text{Mn}$ we observe the NMR spectra of essentially the high-spin isomer, which is prevalent at elevated temperature.¹⁶ Although different signal assignments have been proposed,¹⁷ it has been established by comparing substituted manganocenes¹⁶ and by selective deuteration³ that the signals of D-2-5 of $(\text{MeCp})_2\text{Mn}$ are less shifted than that of the methyl group. D-3/4 and D-2/5 are distinguished by comparison with $(1,2\text{-Me}_2\text{Cp})_2\text{Mn}$ ^{16b}, for which the Cp proton signal of intensity one is more shifted than that of intensity two. It follows that the ligand $s-e_1$ orbital dominates the spin delocalization. Qualitatively, the energy splitting of the ligand e orbitals is the same whether a Cp is substituted by two neighbouring methyl groups or by a single methyl. Therefore, we expect the $s-e_1$ orbital to be also more important for $(\text{MeCp})_2\text{Mn}$, and the signal of D-3/4 to be more shifted than that of D-2/5. This is confirmed by the ^{13}C NMR signal sequence with $\delta^{\text{para}}(\text{C}-1) > \delta^{\text{para}}(\text{C}-3/4) > \delta^{\text{para}}(\text{C}-2/5)$.

Signal half-widths and isotope shifts

Although the signal half-widths could be reduced considerably by using ^2H NMR spectroscopy, the theoretical half-width ratio $W_T(^1\text{H})/W_T(^2\text{H}) = 42.4$ could not be attained. As can be calculated from the data in Table 1 the experimental ratio ranges from 10 to 30. We have previously discussed a number of factors which influence this ratio.¹ In the present study the main problem was the inhomogeneity of the magnetic field, which affected the widths of the deuterium signals more seriously than those of the proton signals.

The primary isotope shifts $\Delta_p^{\text{para}}(^2/1\text{H})$ given in Table 1 are similar to those found earlier for the parent metallocenes Cp_2M .¹ Whenever the error limit of approximately 0.5 ppm is exceeded, the sign of all the isotope shifts of $(\text{MeCp})_2\text{M}$ (and Cp_2M^1 , bearing in mind that we have inverted the sign convention) is the same for a

given M. This is expected when the isotope effect is traced to a change in the overall spin density in the relevant metallocene orbitals on passing from ^1H to ^2H . It is unclear, however, how the isotope shifts depend on the different mechanisms of the spin delocalization.¹

The isotope shifts of $(\text{MeCp})_2\text{Mn}$ are much larger than those of the other metallocenes and they increase with increase in the δ^{para} values (Table 1). The reason for this is that $(\text{MeCp})_2\text{Mn}$ exists as a mixture of high-spin isomers with large signal shifts and low-spin isomers with small signal shifts and partly inverted shift signs.^{3,16b} When the spin crossover experiences an isotope effect, the observed decrease of δ^{para} on going from $(\text{MeCp})_2\text{Mn}$ to $(\text{MeCp})_2\text{Mn}-d_n$ means that the equilibrium of the spin isomers is shifted to the low-spin isomer. We conclude that the slightly higher donor power of deuterium¹⁸ is responsible for the shift of the spin equilibrium. This is in line with the fact that an increasing number of methyl groups per manganocene also favours the low-spin isomer.³ The substituent effect on the spin crossover of manganocenes is so pronounced that it allows not only the detection of a deuterium isotope effect but also the synthesis of derivatives that are pure high- or low-spin species at ambient temperature.^{16b}

EXPERIMENTAL

The 1,1'-dimethylmetallocenes 1-5 were prepared by published procedures^{4c,7a,7c,16b,19} and investigated as mixtures with $(\text{MeCp})_2\text{Fe}$ (ca. 25%, w/w), in 10 mm tubes with ground-glass joints and stoppers, under argon at 338 K. The spectra were recorded on a Bruker MSL 300 spectrometer. All signal shifts and line widths were determined by signal fitting using the Bruker programs incorporated in DISNMR and WINNMR. The MO calculations were carried out using the extended Hückel method using standard parameters for C and H and a modified Wolfsberg-Helmholz expression for calculating H_{ij} off-diagonal elements.²⁰ The atomic parameters for Ni were those obtained previously after charge iteration for Cp_2Ni ,²¹ and the molecular parameters were standard values (C-CH₃ 150 pm, Cp C-H 108 pm, CH₃ C-H 110 pm) or adapted from Cp_2Ni ¹⁴ (Ni-C 216 pm, Cp C-C 140 pm).

Acknowledgement

We thank the Fonds der Chemischen Industrie, Frankfurt, for a Liebig fellowship (J.B.) and for financial support.

REFERENCES

1. N. Hebenanz, F. H. Köhler, F. Scherbaum and B. Schlesinger, *Magn. Reson. Chem.* **27**, 798 (1989).
2. (a) A. Grohmann, F. H. Köhler, G. Müller and H. Zeh, *Chem. Ber.* **122**, 897 (1989); (b) G. A. Luinstra, L. C. ten Cate, H. J. Heeres, J. W. Patiasina, A. Meetsma and J. H. Teuben, *Organometallics* **10**, 3227 (1991).
3. F. H. Köhler and B. Schlesinger, *Inorg. Chem.* **31**, 3853 (1992).
4. (a) H. P. Fritz, H. J. Keller and K. E. Schwarzhan, *Z. Naturforsch., Teil B* **21**, 809 (1966); **22**, 891 (1967); **23**, 293 (1968); (b) M. F. Rettig and R. S. Drago, *J. Am. Chem. Soc.* **91**, 1361 (1969); (c) F. H. Köhler, *J. Organomet. Chem.* **110**, 235 (1976).
5. F. H. Köhler, *Z. Naturforsch., Teil B* **35**, 187 (1980).
6. L. Libit and R. Hoffmann, *J. Am. Chem. Soc.* **96**, 1370 (1974).

7. (a) F. H. Köhler and W. A. Geike, *J. Organomet. Chem.* **328**, 35 (1987); (b) F. H. Köhler and W. A. Geike, *J. Magn. Reson.* **53**, 297 (1983); (c) F. H. Köhler and K. H. Doll, *Z. Naturforsch., Teil B* **37**, 144 (1982).
8. R. S. Drago and H. Petersen, Jr, *J. Am. Chem. Soc.* **89**, 3978 (1967).
9. (a) M. Karplus and G. K. Fraenkel, *J. Chem. Phys.* **35**, 1312 (1961); (b) T. Yonezawa, T. Kawamura and H. Kato, *J. Chem. Phys.*, **50**, 3482 (1969).
10. F. H. Köhler, K. H. Doll and W. Prössdorf, *Angew. Chem.* **92**, 487 (1980); *Angew. Chem., Int. Ed. Engl.* **19**, 479 (1980).
11. R. J. Kurland and B. R. McGarvey, *J. Magn. Reson.* **2**, 286 (1970).
12. P. Baltzer, A. Furrer, J. Hullinger and A. Stebler, *Inorg. Chem.* **27**, 1543 (1988).
13. P. Seiler and J. D. Dunitz, *Acta Crystallogr., Sect. B* **36**, 2255 (1980).
14. J. Blümel, N. Hebindanz, P. Hudeczek, F. H. Köhler and W. Strauss, *J. Am. Chem. Soc.* **114**, 4223 (1992).
15. M. F. Rettig and R. S. Drago, *J. Am. Chem. Soc.* **91**, 3432 (1969).
16. (a) F. H. Köhler and N. Hebindanz, *Chem. Ber.* **116**, 1261 (1983); (b) N. Hebindanz, F. H. Köhler, G. Müller and J. Riede, *J. Am. Chem. Soc.* **108**, 3281 (1986).
17. (a) M. E. Switzer, R. Wang, M. F. Rettig and A. H. Maki, *J. Am. Chem. Soc.* **96**, 7669 (1974); (b) D. Cozak, F. Gauvin and J. Demers, *Can. J. Chem.* **64**, 71 (1986); (c) D. Cozak and F. Gauvin, *Organometallics* **6**, 1912 (1987).
18. E. A. Halevi, *Prog. Phys. Org. Chem.* **1**, 109 (1963).
19. F. H. Köhler, in *Organometallic Syntheses*, edited by R. B. King and J. J. Eisch, Vol. 4, pp. 15, 52 and 96. Elsevier, Amsterdam (1988).
20. (a) R. Hoffmann, *J. Chem. Phys.* **39**, 1397 (1963); (b) R. Hoffmann and W. N. Lipscomb, *J. Chem. Phys.* **36**, 2189 and 2872 (1962); (c) J. H. Ammeter, H.-B. Bürgi, J. C. Thibeault and R. Hoffmann, *J. Chem. Phys.* **100**, 3686 (1978).
21. J. W. Lauher, M. Elian, R. H. Summerville and R. Hoffmann, *J. Am. Chem. Soc.* **98**, 3219 (1976).